The Astrophysical Journal Letters, 724:L122–L126, 2010 November 20 doi:10.1088/2041-8205/724/1/L122

NO EVIDENCE FOR A DARK MATTER DISK WITHIN 4 kpc FROM THE GALACTIC PLANE

C. Moni Bidin[1], G. Carraro[2,5], R. A. Méndez[3], and W. F. van Altena[4]
[1] Universidad de Concepción, departamento de Astronomía, Casilla 160-C, Concepción, Chile; cmbidin@astro-udec.cl
[2] European Southern Observatory, Alonso de Cordova 3107, Vitacura, Santiago, Chile
[3] Universidad de Chile, Departamento de Astronomía, Casilla 36-D, Santiago, Chile
[4] Department of Astronomy, Yale University, P.O. Box 208101, New Haven, CT 06520-8101, USA
Received 2010 April 30; accepted 2010 October 19; published 2010 November 3

ABSTRACT

We estimated the dynamical surface mass density (Σ) at the solar Galactocentric distance between 2 and 4 kpc from the Galactic plane, as inferred from the observed kinematics of the thick disk. We find $\Sigma(z = 2\ \mathrm{kpc}) = 57.6 \pm 5.8\ M_\odot\ \mathrm{pc}^{-2}$, and it shows only a tiny increase in the z range considered by our investigation. We compared our results with the expectations for the visible mass, adopting the most recent estimates in the literature for contributions of the Galactic stellar disk and interstellar medium, and proposed models of the dark matter distribution. Our results match the expectation for the visible mass alone, never differing from it by more than $0.8\ M_\odot\ \mathrm{pc}^{-2}$ at any z, and thus we find little evidence for any dark component. We assume that the dark halo could be undetectable with our method, but the dark disk, recently proposed as a natural expectation of the ΛCDM models, should be detected. Given the good agreement with the visible mass alone, models including a dark disk are less likely, but within errors its existence cannot be excluded. In any case, these results put constraints on its properties: thinner models (scale height lower than 4 kpc) reconcile better with our results and, for any scale height, the lower-density models are preferred. We believe that successfully predicting the stellar thick disk properties and a dark disk in agreement with our observations could be a challenging theoretical task.

Key words: dark matter – Galaxy: kinematics and dynamics – Galaxy: structure

1. INTRODUCTION

Today it is widely accepted that dark matter is a fundamental component of the universe, which plays a key role in the processes of galaxy formation and evolution. Cosmological *N*-body simulations accurately predict the evolution of the dark component and its actual spatial distribution (Moore et al. 1999). In the Λ cold dark matter (ΛCDM) cosmology, spiral galaxies accrete smaller building blocks into both their spheroidal component and their stellar disk. The presence of an old thick disk, very common among spiral galaxies (Dalcanton & Bernstein 2002), is often considered the product of one or more merging events (e.g., Abadi et al. 2003). Lake (1989) first proposed that, as satellites are torn apart by tidal forces, they should deposit their dark matter into a flat dark structure. This idea was recently explored by Read et al. (2008, hereafter Re08), who showed that the presence of a dark disk is a natural expectation of the ΛCDM model. As a result of their simulations, they proposed that a galaxy such as the Milky Way should host a relatively thin dark feature (exponential scale height 2.1–2.4 kpc), with a local density at the solar position (ρ_d) 0.25–1.0 times that of the dark halo (ρ_h). The proposed dark component is much more flattened than the dark halo, but it is still noticeably thicker than any visible disk, because the scale height of the Galactic old thick stellar disk is ∼0.9 kpc, while younger stars and interstellar medium (ISM) form even thinner structures (0.3 and 0.1 kpc, respectively; Jurić et al. 2008).

In the last year it became progressively accepted that if the ΛCDM cosmology is the correct model, dark disks should be ubiquitous in spiral galaxies. More recently, Purcell et al. (2009, hereafter Pu09) elaborated new models, proposing a thicker (scale height 4.6 kpc) but less dense dark disk in the Milky Way ($\rho_\mathrm{d}/\rho_\mathrm{h} \leqslant 0.30$).

[5] Dipartimento di Astronomia, Universitá di Padova, Vicolo Osservatorio 3, I-35122 Padova, Italy.

The presence of a dark disk is strongly related to the formation of the stellar thick disk. However, its merging origin is currently under debate, because of the difficulties of the models in reproducing all its properties. For example, Bournaud et al. (2009) argued that thick disk formation through turbulent and clumpy phases at high redshift can explain its lack of flaring (Momany et al. 2006), at variance with the merger scenario. This model would not necessarily require the presence of a dark disk. On the other hand, the presence of a phantom disk is also an expectation of MOND theory (Milgrom 1983), where the departure of gravitation from Newtonian law should cause the detection of an additional amount of disk matter (Milgrom 2001). It is thus clear that the Milky Way dark disk has become a benchmark for many theories, from gravitational law to cosmological galaxy formation and thick disk origin.

We are performing an extensive survey to study the kinematical and chemical vertical structure of the Galactic thick disk (Carraro et al. 2005). Preliminary results were presented by Moni Bidin et al. (2009). In this Letter, we analyze the vertical trend of the surface mass density as inferred by thick disk kinematics, in search of evidence for any dark component. The detailed analysis of the kinematical results will be published in a later paper (C. Moni Bidin et al. 2011a, in preparation, hereafter Paper I), and the full study of the hypothesis and equations presented here will follow (C. Moni Bidin et al. 2011b, in preparation, hereafter Paper II).

2. OBSERVATIONAL DATA

Our investigation is based on a sample of ∼1200 red giants defined by Girard et al. (2006), vertically distributed with respect to the Galactic plane in a cone of 15 deg radius centered on the south Galactic pole. All objects have Two Micron All Sky Survey (2MASS) photometry (Skrutskie et al. 2006) and absolute proper motions from the SPM3 catalog (Girard et al.

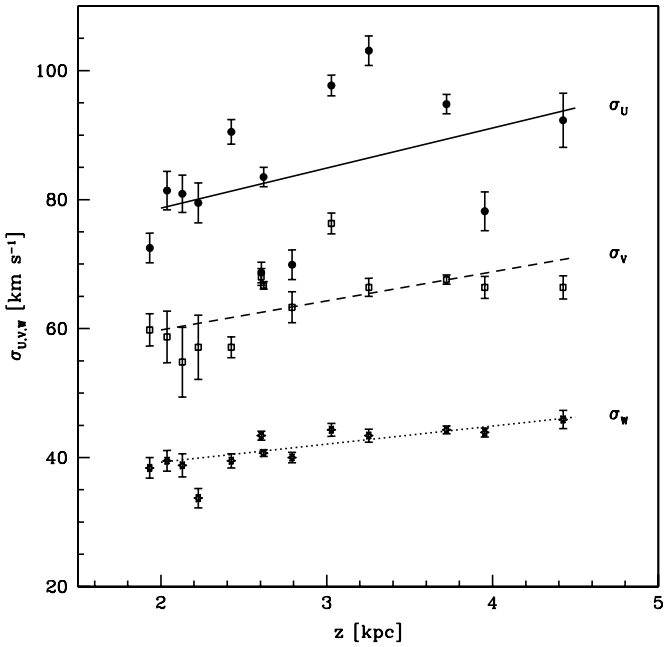

Figure 1. Dispersions of the three velocity components, as a function of Galactic height, and their least-squares fit. Full dots and line: σ_U; open squares and dashed line: σ_V; and open stars and dotted line: σ_W. The errors in z ($\leqslant$100 pc at 4 kpc), given by the statistical error on the mean, are omitted for clarity.

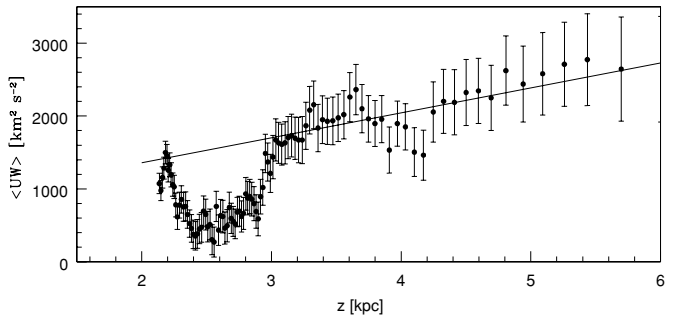

Figure 2. Measured cross-term $\overline{UW}$ as a function of distance from Galactic plane. The line indicates the least-squares fit obtained omitting the depression at 2.5–3 kpc.

2004). The sample was selected by applying a color cut in the infrared color–magnitude diagram to isolate intermediate-metallicity thick disk stars. Main-sequence dwarfs were excluded both by a sloped cut at fainter magnitudes, which excludes all but the nearest ($d \leqslant 63$ pc) dwarfs, and by conservative kinematical criteria imposing a stellar velocity lower than the local escape velocity (550 km s^{-1}; see Girard et al. 2006 for more details). We collected high-resolution Echelle spectra for two-thirds of the Girard et al.'s sample, during 38 nights at La Silla and Las Campanas observatories. The distribution of proper motions and colors of this sub-sample was analyzed to ensure that no selection effect was introduced. We visually inspected all the spectra and excluded the residual low-metallicity stars ([Fe/H]$\leqslant -1.5$), most probably halo contaminators, and misclassified dwarfs. Radial velocities (RVs) were measured for all the stars with a typical error of 0.5–0.7 km s^{-1}, cross-correlating each spectrum with standard stars observed during the same runs (Tonry & Davis 1979). Distances were estimated with a color–absolute magnitude relation calibrated on the red giant branch of 47 Tuc, whose stellar population is very similar to the intermediate-metallicity Galactic thick disk (Wyse & Gilmore 2005). Finally, the three velocity components in the Galactic cylindrical coordinate system (U, V, W), and their associated errors, were calculated for each star from its proper motion, RV, and distance, and the uncertainties on these quantities. The error in distance was $\sim$20% (Moni Bidin 2009), while the error in proper motions was fixed to 3 mas yr^{-1} (T. M. Girard 2009, private communication; see also Girard et al. 2006 for a detailed discussion). The mean errors in (U, V, W) thus increased from $\sim$(7, 36, 38) km s^{-1} at $z = 2$ kpc to $\sim$(10, 61, 66) km s^{-1} at 4 kpc. The details of observations, data reduction, and RV measurements were presented by Moni Bidin (2009), and they will be fully discussed in Paper I.

In this Letter, we restrict our analysis to the $\sim$300 stars beyond 2 kpc from the Galactic plane to avoid contamination by the thin disk. We considered only stars with $|W| \leqslant 150$, $|U| \leqslant 300$, and $-500\,\mathrm{km\,s^{-1}} \leqslant V \leqslant 300$ km s^{-1} to exclude halo stars and/or bad measurements. We did not apply a cut in velocity errors, because it systematically excludes high-velocity stars, biasing the results: the propagation of the uncertainty in distance in fact introduces a term proportional to the velocities themselves. The sample was binned with respect to distance from the Galactic plane z, following three different criteria: three large bins of 85 stars each, five bins of 50, and five of 45 stars. The dispersion in the three velocity components was calculated in each bin, fitting the corresponding probability plot with a linear relation (Lutz & Hanson 1992; see also Bochanski et al. 2007 for an application to a very similar astrophysical case). In the nearest bins ($z \leqslant 2.3$ kpc) the fit was performed outside the $\pm 1\sigma$ range to avoid the residual thin disk contamination (5%–10% according to our estimates). At increasing distance an overestimate was a serious possibility because of some outliers, most probably stars with an incorrect distance and/or proper motion. We consequently excluded from the fit the points on the wings of the distribution showing clear deviation from linearity, i.e., outliers departing from the underlying normal distribution. The mean error in each bin was quadratically subtracted to derive the final estimate of the dispersion. Finally, the dispersion in each velocity component was plotted against the average z of the bin, and a least-squares linear relation was fitted to derive the vertical trend of dispersions.

The results were very similar in the three binning criteria: differences on the derived quantities were smaller than 1.5σ and in most cases agreed within 1σ. We therefore gathered the information of all the bins together, fitting a final plot comprising 13 points. The results are shown in Figure 1. We derive a small vertical gradient of σ_U, σ_V, and σ_W of 6.2 ± 3.7, 4.5 ± 1.9, and 2.8 ± 0.5 km s^{-1} kpc^{-1}, respectively. The statistical uncertainty of the least-square solution was assumed as the error on the linear profile parameters. These could be underestimated because of the correlation of the fitted points, but they are only about 30% higher when fitting the uncorrelated bins of 50 stars, and this has only minimal impact on the final results, because the uncertainties on the thick disk parameters dominate the error budget.

Around $z = 2.5$ kpc we find a sudden deviation from linearity of the cross-term of the dispersion matrix, $\overline{UW}$. This feature could be due to a stellar sub-structure, such as a comoving group of stars. The use of only 13 bins is inadequate to reveal the general trend, hence we binned the data in overlapping groups of 50 stars at steps of 2 stars, as shown in Figure 2. We finally derived the linear relation required for our calculations excluding the "depression" at 2.5 kpc. The line is a good fit outside this feature.

3. THE THEORY

Our formulation is based on the following assumptions.

1. *Steady state*. The thick disk is in equilibrium with the Galactic potential, as expected for an old stellar population. Therefore, all temporal derivatives are set to zero.
2. *Locally flat rotation curve*. The rotation curve is assumed flat at the solar Galactocentric distance.
3. *No net radial or vertical stellar flux*. The mean radial and vertical velocity components are zero, while the rotational component shows a non-null lag (Chiba & Beers 2000; Girard et al. 2006).
4. *Exponential radial dispersion profiles*. All the velocity dispersions decrease with R following an exponential law, with a scale length $h_{R,\sigma}$ equal to the one observed for the mass density ($h_{R,\rho}$).
5. *Vertical constancy of scale lengths*. $h_{R,\rho}$ and $h_{R,\sigma}$ do not depend on z at the solar position. This is observationally verified for the mass density (Cabrera-Lavers et al. 2005), and it is assumed valid for the velocity dispersions, because their radial behavior is linked to the mass distribution by assumption (4).
6. *Null cross term on the Galactic plane*. $\overline{UW}\,(z = 0) = 0$. This hypothesis is required for symmetry reasons (see, e.g., Bienaymé 2009), and it is observationally confirmed by Fuchs et al. (2009).

The hypothesis (4) is observationally confirmed for σ_W (van der Kruit & Searle 1982). Its extension to the other components relies on the controversial assumption of constant anisotropy, i.e., $\frac{\partial}{\partial R}\frac{\sigma_U}{\sigma_W} = 0$. We have no information about the radial trend of the velocity dispersions, but this assumption is supported by observations (Lewis & Freeman 1989) and numerical simulations for $R \leqslant 9$ kpc (Cuddeford & Amendt 1992).

Integrating the Poisson equation from $-z$ to z, assuming that the vertical component of the force F_z is null on the plane, we obtain

$$-2\pi G\Sigma(z) = \int_0^z \frac{1}{R}\frac{\partial}{\partial R}(RF_{\rm R})dz + F_z(z), \quad (1)$$

where $\Sigma(z)$ is the surface mass density between $\pm z$ and $F_{\rm R}$ is the radial component of the force. Inserting the Jeans equations in Equation (1), making use of our hypotheses (1)–(6) and calculating simple derivatives and integrals, we eventually obtain the final expression:

$$\Sigma(z) = \frac{1}{2\pi G}\left[k_1 \cdot \int_0^z \sigma_U^2 dz + k_2 \cdot \int_0^z \sigma_V^2 dz + k_3 \cdot \int_0^z \overline{UW} dz + k_4 \cdot \overline{UW} + \frac{\sigma_W^2}{h_{z,\rho}} - \frac{\partial \sigma_W^2}{\partial z}\right], \quad (2)$$

where $h_{z,\rho}$ is the thick disk exponential scale height, and

$$k_1 = \frac{3}{R_\odot \cdot h_{R,\rho}} - \frac{2}{h_{R,\rho}^2}, \quad (3)$$

$$k_2 = -\frac{1}{R_\odot \cdot h_{R,\rho}}, \quad (4)$$

$$k_3 = -\frac{1}{h_{z,\rho}} \cdot \left(\frac{1}{R_\odot} - \frac{1}{h_{R,\rho}}\right), \quad (5)$$

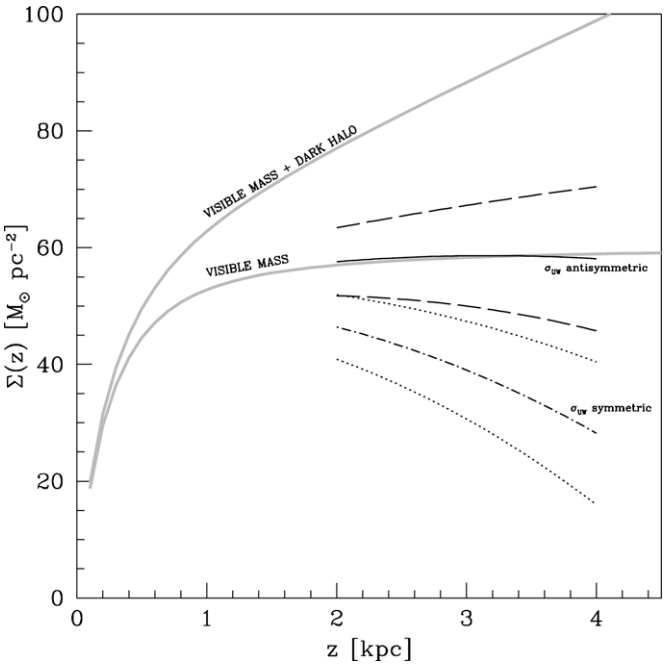

Figure 3. Surface density vertical profile derived from our observations. The full line shows the results under the assumption of cross-term antisymmetry, while the dash-dotted line indicates the results for a symmetric cross-term. The dashed and dotted lines indicate the corresponding 1σ strips. Light gray curves represent the expectations of the visible mass alone (lower curve) and of a visible mass+dark halo model (upper curve).

$$k_4 = \frac{3}{h_{R,\rho}} - \frac{2}{R_\odot}. \quad (6)$$

To calculate the surface density we must insert into Equation (2) the vertical trends of the kinematical quantities σ_U, σ_V, σ_W, and $\overline{UW}$ plus the three parameters $R_\odot$, $h_{z,\rho}$, and $h_{R,\rho}$. We fixed $R_\odot = 8.0 \pm 0.3$ kpc and defined the thick disk scale height and length as the mean of about 20 literature estimates (see Moni Bidin 2009, and Paper II for the bibliographical references), obtaining $h_{R,\rho} = 3.8 \pm 0.2$ kpc and $h_{z,\rho} = 0.90 \pm 0.08$ kpc. The quoted errors are given by the error on the mean that should be the most appropriate statistic when averaging many uncorrelated measurements. However, they could be too small because of the traditional uncertainty on these parameters, although the estimates converged considerably in the last years. We therefore also considered an uncertainty of 0.4 and 0.12 kpc, respectively, comprising all the measurements of the last decade within $\pm 2\sigma$ ($\sim$70% within $\pm 1\sigma$). These larger errors necessarily decrease the significance of the results, but without altering the general conclusions, as can be deduced from Figure 4. The error on $\Sigma(z)$ was calculated from the propagation of errors of all the quantities in Equation (2).

In deriving Equation (2), we assumed the kinematical quantities as symmetric with respect to the plane, so that their integrals between $-z$ and z are twice the product of integration between 0 and z. This is easily justified for the dispersions, but it may not be the case for $\overline{UW}$. We therefore also considered an antisymmetric cross-term, where the third term of Equation (2) vanishes. As shown in Figure 3, a symmetric cross-term fails to return physically meaningful results, because it violates two minimum requirements: the surface density must at least account for the known visible matter, and it cannot decrease with z. We will therefore assume the cross-term as antisymmetric and consider only the results obtained under this hypothesis hereafter.

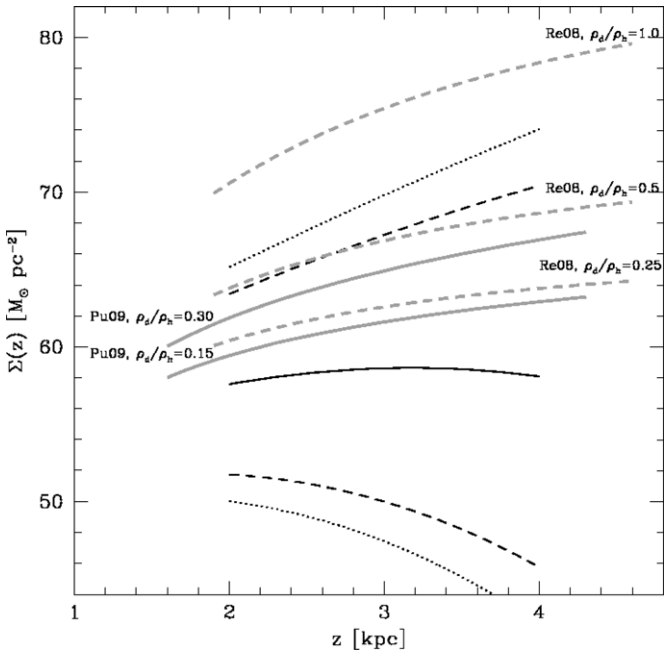

Figure 4. Comparison of our results with the expectations of dark disk models. The black full line shows the observational result with its 1σ errors (dashed lines) as in Figure 3. The dotted lines indicate the 1σ strip when the enhanced errors on the thick disk parameters, discussed in the text, are considered. The light gray curves are models where a dark disk is added to the visible mass, based on the models proposed by Re08 (dashed lines, $h_{z,D} = 2.4$ kpc and three different values of local density) and by Pu09 (full line, $h_{z,D} = 4.6$ kpc, two values of local density).

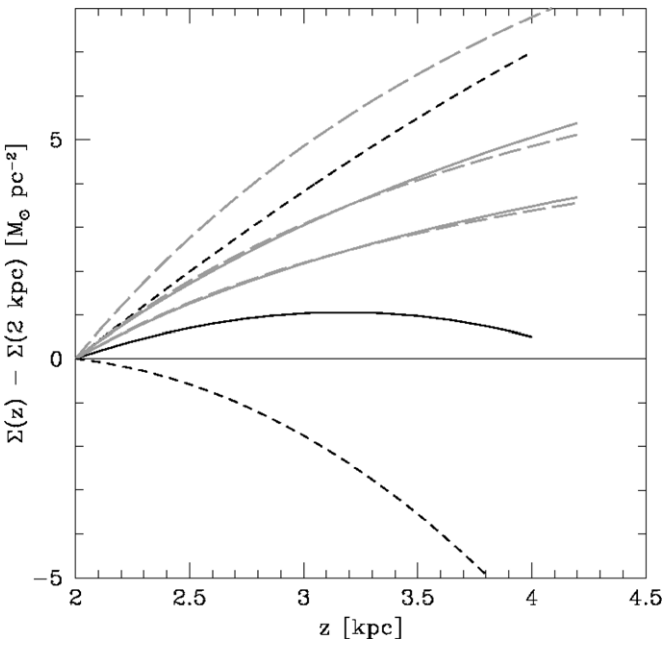

Figure 5. Same as Figure 4, but for the increment of the surface mass density as a function of z, with respect to 2 kpc, instead of its absolute value.

4. RESULTS

Our results are shown in Figure 3. We find $\Sigma(2\ \mathrm{kpc}) = 57.6 \pm 5.8\ M_\odot\ \mathrm{pc}^{-2}$, and the curve is nearly flat in the whole range, while the error increases constantly to $\sim 12\ M_\odot\ \mathrm{pc}^{-2}$ at 4 kpc. The solution increases $1\ M_\odot\ \mathrm{pc}^{-2}$ between 2 and 3.2 kpc, then it turns slightly downward. However, the decrease is so small ($0.55\ M_\odot\ \mathrm{pc}^{-2}$) that a small refinement of any parameter would correct it, for example, increasing $h_{R,\rho}$ by 0.1 kpc. Moreover, this problem is present only in the lower half of the family of solutions defined by the $\pm 1\sigma$ strip. We did not alter the input parameters to amend it, because this would add a high degree of arbitrariness to the results.

In Figure 3, we overplot a model of surface mass density due to the visible mass. The thin and thick disk exponential scale heights, the halo shape, and the local thick disk and halo normalization were taken from Jurić et al. (2008). We included a thin layer (100 pc) of ISM contributing $13\ M_\odot\ \mathrm{pc}^{-2}$ (Holmberg & Flynn 2000), and the thin disk density on the plane was normalized by the requirement $\Sigma_{\mathrm{disk}}\ (1.1\ \mathrm{kpc}) = 40\ M_\odot\ \mathrm{pc}^{-2}$ (Holmberg & Flynn 2004). This quantity includes all disk stellar components and remnants, and it is currently the best estimate often assumed in Galactic mass models (Dehnen &Binney 1998; Olling & Merrifield 2001; Weber & de Boer 2010).

The agreement between the visible mass and our dynamical solution is striking, and there is no need to invoke any dark component. In Figure 3, we also plot a model including a dark halo (Olling & Merrifield 2001). The curve is completely incompatible with our results, both for its high value and steep slope. One can argue that we are actually deducing the mass from the change in the gravitation potential: the dark halo could be too uniform and extended to cause a detectable change on stellar kinematics in a range of 4 kpc. This point requires a detailed analysis that is beyond the scope of this Letter, and we leave it to a later study (Paper II). Here, we assume that the dark halo is undetectable and focus on the dark disk, for which this explanation is not viable.

Figure 4 compares our results with models where a dark disk is considered. They require the definition of two additional parameters: the exponential scale height of the dark component $h_{z,D}$ and its density at $z = 0$, normalized with respect to the dark halo, $\rho_{\mathrm{d}}/\rho_{\mathrm{h}}$. We considered two families of models: a relatively thinner ($h_{z,D} = 2.4$ kpc) dark disk with $\rho_{\mathrm{d}}/\rho_{\mathrm{h}} = 0.25$–$1.0$, as proposed by Re8, and a thicker, less dense one ($h_{z,D} = 4.6$ kpc, $\rho_{\mathrm{d}}/\rho_{\mathrm{h}} = 0.15$–$0.30$) from Pu09. The measured surface density matches the baryonic mass alone, and any curve including the dark disk departs from the central solution, being therefore less likely. Hence, there is no evidence for a flattened dark component, but its expected contribution is small compared to the errors and its existence cannot be completely ruled out. However, not all combinations of dark disk parameters are permitted by our observations: the Pu09 solutions fall in the 1σ strip, but only the less dense models of Re08 do. This is entirely due to the lower densities of the first family of models. In fact, for a fixed $\rho_{\mathrm{d}}/\rho_{\mathrm{h}}$, the thick Pu09 models depart more from the observed curve, and they require a higher increment of $\Sigma(z)$ compared to Re08 models (see Figure 5). We can thus derive important constraints: a lower density is favored in all cases, and thinner disks should be preferred, while thick and dense dark disks ($h_{z,D} \geqslant 4$ kpc, $\rho_{\mathrm{d}}/\rho_{\mathrm{h}} \geqslant 0.5$) are less likely. Numerical simulations showed that low-latitude merging of massive satellites are required to form a heated disk kinematically similar to the Galactic thick disk (Villalobos & Helmi 2009), but these events produce denser dark disks (Pu09). In addition, Re08 showed that the observed density of the stellar thick disk can be reproduced only by a few models, all implying a more massive dark disk ($\rho_{\mathrm{d}}/\rho_{\mathrm{h}} \geqslant 0.4$). In summary, correctly predicting the thick disk kinematical and dark disk properties is a challenging task. Models for thick disk formation alternative to the merging scenario (e.g., Bournaud et al. 2009) are preferred,

while the MONDian prediction of Bienaymé et al. (2009), i.e., a 60% increase of disk mass due to a phantom disk ($\sim$30 $M_\odot$ pc^{-2} at 2 kpc), is in contradiction with our results.

It could be argued that our model of visible mass, it relies on poorly constrained quantities, such as the ISM contribution and $\Sigma_{\rm disk}$(1.1 kpc), and a downward correction of these parameters would shift all the model curves to lower values. Therefore, in Figure 5 we analyzed both the expected and measured increment of $\Sigma(z)$, i.e., the surface density of the mass comprised between z and 2 kpc. This quantity is completely independent of the ISM at these Galactic heights, and the assumed value of $\Sigma_{\rm disk}$(1.1 kpc) introduces a negligible uncertainty ($\leqslant$0.15 $M_\odot$ pc^{-2}). Figure 5 shows exactly the same situation analyzed previously, and our conclusions should be considered independent of the details and uncertainties of the modeled visible mass.

5. CONCLUSIONS

We estimated the Galactic surface mass density between 2 and 4 kpc from the plane, finding $\Sigma(2\ {\rm kpc}) = 58 \pm 6\ M_\odot\ {\rm pc}^{-2}$, and a nearly flat curve. Our results strikingly match the visible mass alone, and we do not detect evidence for any dark component, although the dark halo could have passed unseen. There is no compelling evidence for a dark disk, but within the errors of our investigation, its existence cannot be completely excluded. We derive important constraints on its expected properties: lower densities ($\rho_{\rm d}/\rho_{\rm h} \leqslant 0.25$) should be preferred in any case, and a thin dark disk ($h_{z,D} \leqslant 2.5$ kpc) better reconciles with observations. A thick and dense dark disk ($h_{z,D} \geqslant 4$ kpc, $\rho_{\rm d}/\rho_{\rm h} \geqslant 0.5$) should be excluded. Any merging model aiming to reproduce the formation of the Galactic thick disk and a flat dark component will need to consider the constraints from our investigation.

The authors are grateful to V. Korchagin for his assistance. C.M.B. acknowledges the Chilean Centro de Excelencia en Astrofísica y Tecnologías Afines (CATA), D. Geisler for his reading of the manuscript, and F. Mauro for useful discussions. R.A.M. acknowledges support by the Chilean Centro de Astrofisica FONDAP (No. 15010003), FONDECYT (No. 1070312), and by CATA (PFB-06). All authors acknowledge partial support from the Yale University/Universidad de Chile collaboration. The SPM3 catalog was funded in part by grants from the US National Science Foundation, Yale University, and the Universidad Nacional de San Juan, Argentina.

Facilities: Du Pont (ECHELLE), Magellan:Clay (MIKE), Euler1.2m (CORALIE), Max Planck:2.2m (FEROS)

REFERENCES

Abadi, M. G., Navarro, J. F., Steinmetz, M., & Eke, V. R. 2003, ApJ, 597, 21
Bienaymé, O. 2009, A&A, 500, 781
Bienaymé, O., Famaey, B., Wu, X., Zhao, H. S., & Aubert, D. 2009, A&A, 500, 801
Bochanski, J. J., Munn, J. A., Hawley, S. L., West, A. A., Covey, K. R., & Schneider, D. P. 2007, AJ, 134, 2418
Bournaud, F., Elmegreen, B. G., & Martig, M. 2009, ApJ, 707, L1
Cabrera-Lavers, A., Garzón, F., & Hammersley, P. L. 2005, A&A, 433, 173
Carraro, G., van Altena, W. F., Moni Bidin, C., Girard, T. M., Méndez, R. A., Dinescu, D. I., & Korchagin, V. I. 2005, BAAS, 37, 1378
Chiba, M., & Beers, T. C. 2000, AJ, 119, 2843
Cuddeford, P., & Amendt, P. 1992, MNRAS, 256, 166
Dalcanton, J. J., & Bernstein, R. A. 2002, AJ, 124, 1328
Dehnen, W., & Binney, J. 1998, MNRAS, 294, 429
Fuchs, B., et al. 2009, AJ, 137, 4149
Girard, T. M., Dinescu, D. I., van Altena, W. F., Platais, I., Monet, D. G., & López, C. E. 2004, AJ, 127, 3060
Girard, T. M., Korchagin, V. I., Casetti-Dinescu, D. I., van Altena, W. F., López, C. E., & Monet, D. G. 2006, AJ, 132, 1768
Holmberg, J., & Flynn, C. 2000, MNRAS, 313, 209
Holmberg, J., & Flynn, C. 2004, MNRAS, 352, 440
Jurić, M., et al. 2008, ApJ, 673, 864
Lake, G. 1989, AJ, 98, 1554
Lewis, J. R., & Freeman, K. C. 1989, AJ, 97, 139
Lutz, T. E., & Hanson, R. B. 1992, in ASP Conf. Ser. 25, Astronomical Data Analysis Software and Systems I, ed. D. M. Worrall, C. Biemesderfer, & J. Barnes (San Francisco, CA: ASP), 257
Milgrom, M. 1983, ApJ, 270, 371
Milgrom, M. 2001, MNRAS, 326, 1261
Momany, Y., Zaggia, S., Gilmore, G., Piotto, G., Carraro, G., Bedin, L. R., & De Angeli, F. 2006, A&A, 451, 515
Moni Bidin, C. 2009, PhD thesis, Universidad de Chile
Moni Bidin, C., Girard, T. M., Carraro, G., Méndez, R. A., van Altena, W. F., Korchagin, V. I., & Dinescu, D. I. 2009, RevMexAAC, 35, 109
Moore, B., Ghigna, S., Governato, F., Lake, G., Quinn, T., Stadel, J., & Tozzi, P. 1999, ApJ, 524, L19
Olling, R. P., & Merrifield, M. R. 2001, MNRAS, 326, 164
Purcell, C. W., Bullock, J. S., & Kaplinghat, M. 2009, ApJ, 703, 2275
Read, J. I., Lake, G., Agertz, O., & Debattista, V. P. 2008, MNRAS, 389, 1041
Skrutskie, M. F., et al. 2006, AJ, 131, 1163
Tonry, J., & Davis, M. 1979, AJ, 84, 1511
van der Kruit, P. C., & Searle, L. 1982, A&A, 110, 61
Villalobos, A., & Helmi, A. 2009, MNRAS, 399, 166
Weber, M., & de Boer, W. 2010, A&A, 509, 25
Wyse, R. F. G., & Gilmore, G. 2005, arXiv:astro-ph/0510025